Deconvolution and correlation-based interferometric redatuming by wavefield inversion

Diego F. Barrera, J. Schleicher†, J. van der Neut‡ and K. Wapenaar‡*
**DEP/UNICAMP & INCT-GP, †IMECC/UNICAMP & INCT-GP and ‡Delft University of Technology*

SUMMARY

Seismic interferometry is a method to retrieve Green's functions for sources (or receivers) where there are only receivers (or sources, respectively). This can be done by correlation- or deconvolution-based methods. In this work we present a new approach to reposition the seismic array from the earth's surface to an arbitrary datum at depth using the one-way reciprocity theorems of convolution and correlation type. The redatuming process is done in three steps: (a) retrieving the downward Green's function for sources at the earth's surface and receivers at the datum, (b) retrieving the corresponding upward Green's function, and (c) retrieving the reflected upward wavefield for sources and receivers at the datum. Input for steps (a) and (b) are the surface data and wavefields simulated in a velocity model of the datum overburden. Step (c) uses the responses of steps (a) and (b) as input data in the convolution-based interferometric equation. The method accounts for inhomogeneities in the overburden medium, thus reducing anticausal events and artefacts as compared to a purely correlation-based procedure.

INTRODUCTION

Seismic interferometry is a technique that allows to retrieve Green's functions for sources at positions where only receivers are available (or vice versa). The classic redatuming procedure correlates surface seismic data with those acquired at depth. This correlation-based method has been well studied in the literature, e.g., by Wapenaar et al. (2008), Schuster (2009), Curtis (2009), Wapenaar et al. (2010), van der Neut (2012).

Seismic interferometry by deconvolution is an alternative to the classical correlation-based scheme. There are many situations where the deconvolutional form is more convenient than the correlation based methods. One of the main advantages of the deconvolution-based procedure is its inherent compensation for the properties of the source wavelet. Another important advantage is that the underlying theory does not require the assumtion of a lossless medium (Slob and Wapenaar, 2007).

In this work, we combine deconvolution-based interferometry with inverse wavefield extrapolation to derive an alternative procedure for retrieving the total wavefield at the datum. Inverse wavefield extrapolation is a concept used to describe the process of retrieving the focusing functions at an arbitrary datum by means of retropropagation of the wavefield recorded at the earth's surface (van der Neut et al., 2015b). In our proposed procedure, we use a convenient form of inverse wavefield extrapolation to determine the down- and upward propagating Green's function at the datum for a point source at the earth's surface. This down- and upgoing Green's function is then used to retrieve the complete wavefield at the datum, free from interactions with the part of the medium above the redatuming level. Using this new approach, we reduce the influence of the overburden in the form of multiples, spurious events of the Green's functions, and anticausal events. The only required information for the proposed technique is a velocity model of the datum overburden. This model is used to simulate the vertical derivative of the transmitted wavefield to the datum and the truncated overburden-scattered wavefield at the surface and its cossresponding vertical derivative.

RECIPROCITY THEOREMS OF CONVOLUTION AND CORRELATION TYPE

We consider two states A and B in the Helmholtz equation in order to calculate the reciprocity theorem of the convolution type. We assume that inside some volume V, both states have the same properties, i.e., $\rho^A(x) = \rho^B(x) = \rho(x)$ and $c^A(x) = c^B(x) = c(x)$. Since the states differ only in the source, corresponding wavefields p^A and p^B must satisfy

$$\rho(x)\nabla \cdot \left[\frac{1}{\rho(x)}\nabla \hat{p}^A\right] + \frac{\omega^2}{c^2(x)}\hat{p}^A = -\hat{S}^A, \qquad (1)$$

$$\rho(x)\nabla \cdot \left[\frac{1}{\rho(x)}\nabla \hat{p}^B\right] + \frac{\omega^2}{c^2(x)}\hat{p}^B = -\hat{S}^B. \qquad (2)$$

Here $\rho(x)$ denotes the variable density, $\hat{p}$ the pressure field, $c(x)$ is the spatially varying wave velocity and $\hat{S}(x,\omega)$ is a source term. Equations (1) and (2) allow to deduce the reciprocity theorem of convolution type as

$$\oiint_{\partial V} \frac{1}{\rho(x)}\left(\hat{p}^B\nabla\hat{p}^A - \hat{p}^A\nabla\hat{p}^B\right)\cdot\hat{n}ds = \iiint_V \frac{1}{\rho(x)}\left(\hat{p}^A\hat{S}^B - \hat{p}^B\hat{S}^A\right)dv, \qquad (3)$$

where ∂V is the boundary of V and ds is the infinitesimal element on ∂V. A completely analogous analysis can be carried out starting at the complex conjugate of equation (1) together with equation (2). Replacing the wavefield $\hat{p}^A$ and the source term $\hat{S}^A$ in the above derivation by their complex conjugates $\hat{p}^{A*}$ and $\hat{S}^{A*}$, where the superscript * denotes the complex conjugate, results in

$$\oiint_{\partial V} \frac{1}{\rho(x)}\left(\hat{p}^B\nabla\hat{p}^{A*} - \hat{p}^{A*}\nabla\hat{p}^B\right)\cdot\hat{n}ds = \iiint_V \frac{1}{\rho(x)}\left(\hat{p}^{A*}\hat{S}^B - \hat{p}^B\hat{S}^{A*}\right)dv. \qquad (4)$$

This is the reciprocity theorem of correlation type, which is independent of the actual shape of volume V. Considering that are no sources inside volume V, the right-hand sides of equations (3) and (4) vanish. To analyze the closed-surface integral, we consider a cylindrical shape, where the surface ∂V is decomposed into three parts. We note that at infinite radius, the integral over the cylinder mantle does not contribute (Wapenaar and Berkhout, 1989). Denoting the top part of the cylinder surface as that $\partial V_1 = \left\{(x_1,x_2,x_3)\in\mathbb{R}^3 | x_3 = x_3^1\right\}$ and the bottom surface as $\partial V_2 = \{(x_1, x_2, x_3) \in \mathbb{R}^3 | x_3 = x_3^2\}$, we can rewrite expressions (3) and (4) as

$$\iint_{\partial V_1} \frac{1}{\rho(x)} (\hat{p}^B \nabla \hat{p}^A - \hat{p}^A \nabla \hat{p}^B) \cdot \hat{n}_1 dx_1 dx_2 = - \iint_{\partial V_2} \frac{1}{\rho(x)} (\hat{p}^B \nabla \hat{p}^A - \hat{p}^A \nabla \hat{p}^B) \cdot \hat{n}_2 dx_1 dx_2. \tag{5}$$

and

$$\iint_{\partial V_1} \frac{1}{\rho(x)} (\hat{p}^B \nabla \hat{p}^{A*} - \hat{p}^{A*} \nabla \hat{p}^B) \cdot \hat{n}_1 dx_1 dx_2 = - \iint_{\partial V_2} \frac{1}{\rho(x)} (\hat{p}^B \nabla \hat{p}^{A*} - \hat{p}^{A*} \nabla \hat{p}^B) \cdot \hat{n}_2 dx_1 dx_2. \tag{6}$$

According to Wapenaar and Berkhout (1989) the total wave field can be decomposed in down- $(+)$ and up-going $(-)$ constituents, as

$$\hat{p}(x, \omega) = \hat{p}_+(x, \omega) + \hat{p}_-(x, \omega). \tag{7}$$

Substitution of decomposition (7) in expressions (5) and (6) with the normal vectors at surfaces ∂V_1 and ∂V_2 as $\hat{n}_1 = (0, 0, -1)$ and $\hat{n}_2 = (0, 0, 1)$, respectively, we obtain the one-way reciprocity theorems of convolution and correlation type, respectively (Wapenaar and Fokkema, 2006), that are written conveniently as

$$\iint_{\partial V_1} \frac{1}{\rho(x)} \left[\hat{p}_-^B \partial_3 \hat{p}_+^A - \hat{p}_-^A \partial_3 \hat{p}_+^B\right] dx_1 dx_2 = \iint_{\partial V_2} \frac{1}{\rho(x)} \left[\hat{p}_-^B \partial_3 \hat{p}_+^A - \hat{p}_-^A \partial_3 \hat{p}_+^B\right] dx_1 dx_2. \tag{8}$$

and

$$\iint_{\partial V_1} \frac{1}{\rho(x)} \left[\hat{p}_-^B \partial_3 \hat{p}_-^{A*} - \hat{p}_+^{A*} \partial_3 \hat{p}_+^B\right] dx_1 dx_2 = \iint_{\partial V_2} \frac{1}{\rho(x)} \left[\hat{p}_+^B \partial_3 \hat{p}_+^{A*} + \hat{p}_-^B \partial_3 \hat{p}_-^{A*}\right] dx_1 dx_2. \tag{9}$$

DOWN- AND UPWARD GREEN'S FUNCTIONS

Using the reciprocity theorems of convolution and correlation type, it is possible to retrieve the up- and downward propagating wavefields at an arbitrary datum in depth. For this purpose, we still need an additional relationship, previously derived by van der Neut et al. (2015a). To derive this relationship in our notation, we start again at two states, A and B (indicated by superscripts A and B) in the frequency-space domain (see Figure 1).

In state A, we consider a monopole point source positioned immediately above surface ∂V_1. In this situation, the vertical derivative of the downgoing wavefield at the surface can be expressed as $\partial_3 \hat{p}_+^A = -\frac{1}{2}\delta(x_1 - x_1^A)\delta(x_2 - x_2^A)$ (Wapenaar et al., 2014). The validity region of this expression in state A is limited by surfaces ∂V_1 and ∂V_2. Between these surfaces, the medium may be arbitrarily inhomogeneous. Above ∂V_1

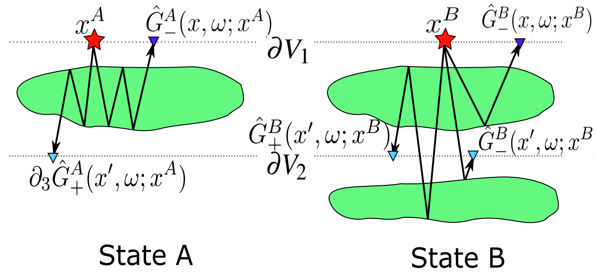

Figure 1: Two wavefield states in an inhomogeneous overburden. State A is used to describe the transmitted wavefield from the surface and it responses recorded at the datum and at the surface. State B is used to describe the total wavefield taking into account all events propagating in the medium.

and below ∂V_2 we consider homogeneous halfspaces without a free surface (Figure 1).

In state B, we consider the same inhomogeneous medium between surfaces ∂V_1 and ∂V_2 as in state A. Above ∂V_1, we still consider a homogeneous medium halfspace without a free surface, and below ∂V_2 we now consider a scattering body. The source in state B is also a point source immediately above surface ∂V_1, such that the vertical derivative of the downgoing wavefield can be represented as $\partial_3 \hat{p}_+^B = -\frac{1}{2}\delta(x_1 - x_1^B)\delta(x_2 - x_2^B)$ (Wapenaar et al., 2014). In both states A and B, we consider the wavefield decomposition into up- and downgoing constituents in analogy to equation (7). An analysis of the physical situation in both states allows for an interpretation of all propagating events at every surface in Figure 1, resulting in Table 1.

Table 1: Analysis of the up- and downgoing wavefields at surfaces ∂V_1 and ∂V_2 in states A and B, respectively.

Surface	Direction	Wavefield in State A	Wavefield in State B
∂V_1	+	point source in x^A	point source in x^B
∂V_1	-	$\hat{G}_-^A(x,\omega;x^A)$	$\hat{G}_-^B(x,\omega;x^B)$
∂V_2	+	$\hat{G}_+^A(x',\omega;x^A)$	$\hat{G}_+^B(x',\omega;x^B)$
∂V_2	-	0	$\hat{G}_-^B(x',\omega;x^B)$

Substitution of the wavefield expressions from Table 1 in the one-way reciprocity theorem of convolution type in equation (8) leads to

$$\frac{1}{\rho(x^A)} \hat{G}_-^B(x^A, \omega; x^B) - \frac{1}{\rho(x^B)} \hat{G}_-^A(x^B, \omega; x^A) = -2 \iint_{\partial V_2} \frac{1}{\rho(x)} \hat{G}_-^B(x', \omega; x^B) \partial_3 \hat{G}_+^A(x', \omega; x^A) d^2x', \tag{10}$$

where we have also used that the vertical wavefield derivatives at the point sources are given by delta functions as mentioned above. Equation (10) is an expression that allows for least-squares inversion to retrieve the up-going Green's function $\hat{G}_-^B(x', \omega; x^B)$ in State B (i.e., for the complete inhomogeneous medium) if we know the terms $\frac{1}{\rho(x^B)}\hat{G}_-^A(x^B, \omega; x^A)$ and $\frac{1}{\rho(x)}\partial_3 \hat{G}_+^A(x', \omega; x^A)$ in State A (which uses only a model of the inhomogeneities in between the surfaces ∂V_1 and ∂V_2).

In analogy to this analysis, we can replace the wavefield expressions of Table 1 in the one-way reciprocity theorem of correlation type in equation (9). This leads to

$$\iint_{\partial V_1} \frac{1}{\rho(x)} \hat{G}_-^B(x,\omega;x^B)\partial_3 \hat{G}_-^{A*}(x,\omega;x^A) d^2x + \frac{1}{2\rho(x^B)} \hat{G}_+^{A*}(x^B,\omega;x^A) = -\iint_{\partial V_2} \frac{1}{\rho(x)} \hat{G}_+^{A*}(x',\omega;x^A)\partial_3 \hat{G}_+^B(x',\omega;x^B) d^2x'. \quad (11)$$

Equation (11) allows us to calculate the vertical derivative of the downgoing Green's function $\partial_3 \hat{G}_+^B(x',\omega;x^B)$ at the datum, if we know the complex conjugate of the transmitted wavefield $\frac{1}{\rho(x)}\hat{G}_+^{A*}(x',\omega;x^B)$ from the earth's surface until the datum in state A. We also need to know the complex conjugate of the downgoing wavefield $\frac{1}{\rho(x^B)}\hat{G}_+^{A*}(x^B,\omega;x^A)$ over the surface ∂V_1 and the vertical derivative of the complex conjugate of the truncated upgoing wavefield $\frac{1}{\rho(x)}\partial_3 \hat{G}_-^{A*}(x,\omega;x^A)$ in state A.

REDATUMING

The above equations allow for retrieving the down- and upgoing constituents of the Green's functions for sources at the surface and receivers at the datum. Therefore, we still need an equation to redatum the sources. For this purpose, we note that each trace in the output gather $\hat{G}_-^B(x',\omega;x^B)$ can be interpreted as the stack of a convolution gather, which is obtained by deconvolution of each trace in the reflection response $\hat{R}_n(x'',\omega;x')$ at a fixed source point x' at the datum with each trace of the vertical derivative of the downgoing constituent $\partial_3 \hat{G}_+^B(x',\omega;x^B)$ for a fixed source position x^B at surface and receiver positions x' at the datum. Mathematically, the deconvolution-based redatuming equation can be expressed in the case of variable density as

$$\frac{1}{\rho(x')}\hat{G}_-^B(x',\omega;x^B) = -2\rho(x')\iint_{\partial V_2} \frac{1}{\rho(x)} \hat{R}_n(x'',\omega;x')\partial_3 \hat{G}_+^B(x',\omega;x^B) d^2x''. \quad (12)$$

Figure 2 explains this linear inversion problem graphically.

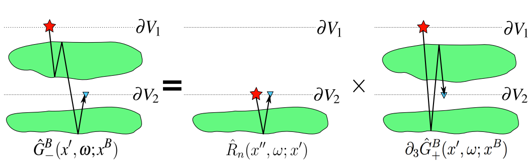

Figure 2: Sketch explaining the linear inversion problem (12). Once the one-way Green's functions responses at the datum have been determined in the previous steps, the reflected wavefield at the datum can be calculated by inversion.

Equation (12) completes the procedure proposed in this work. with this equation, it is possible to retrieve the total wavefield at the datum $\hat{R}_n(x'',\omega;x')$ using any inversion method (in this work we used stabilized least-squares inversion), if we know the up- and downward Green's function constituents $\frac{1}{\rho(x')}\hat{G}_-^B(x',\omega,x^B)$ and $\frac{1}{\rho(x)}\hat{G}_+^B(x',\omega;x^B)$.

RESULTS

In this numerical example, we demonstrate and interpret the main result of this work. To do so, we used a horizontal-layered velocity model with a width of 8 km and a depth of 2 km containing velocities between 1.8 km/s and 2.5 km/s. The datum is located at 500 m depth. The acquisition models has 201 sources spaced at 25 m and the same number of receivers for each shot located at the earth's surface and in the datum. Using these data and the true velocity model of the datum overburden, we determine the down- and upward wavefield constituents for receivers at depth, and then the redatumed wavefield with sources and receivers at the datum.

For the redatuming, we needed to simulate the following wavefields in the overburden model: (a) the transmitted wavefield from the earth's surface at the datum in 500 m in depth and its corresponding vertical derivative, and (b) the truncated reflected wavefield with source and receivers at the earth's surface and its corresponding vertical derivative.

For comparison, we simulated the full wavefield (Figure 3a) with sources at the surface and receivers at the datum. The visible events are labeled with numbers in order to identify and interpret them. Figure 3b and c show the ray paths of the down- and upgoing events, respectively, and the corresponding labels. To facilitate the interpretation, we use green arrows for downgoing events and red arrows for upgoing events. This also helps us to compare the respective events with the inverted down- and upgoing wavefield constituents shown below.

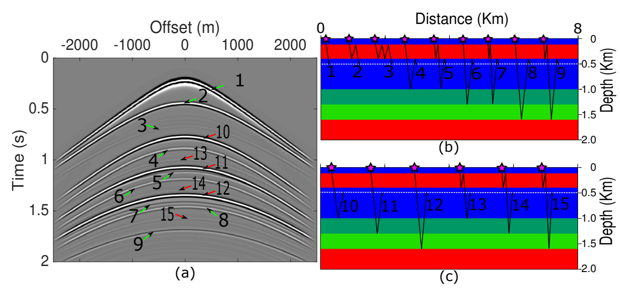

Figure 3: (a) Full synthetic seismic wavefield labeled with the ray paths of its (b) down- and (c) upgoing constituents at the datum in 500 m depth.

An important aspect of all steps of our numerical inversion, i.e., the retrieval of the down- and upward Green's functions, and the full reflected wavefield for sources and receivers at datum, is that we actually invert a point spread function (PSF). Using a damped least-squares scheme to retrieve the inverse of the PSF, we tested different values of the regularization parameter ε in the inverse process. We used for ε different percentage values with respect to the maximum value of the PSF. Figures 4, 5, and 6 show the inversion results for the percentages: (a) 0.1% and (b) 0.01%.

Figure 4 shows the Green's function $\hat{G}_+^B(x',\omega;x^B)$ at the datum in 500 m depth, inverted using equation (11), for the indicated values of the regularization parameters. In both sections, the kinematic properties and the relative amplitudes nicely match those of the downward propagating events in Figure 3a.

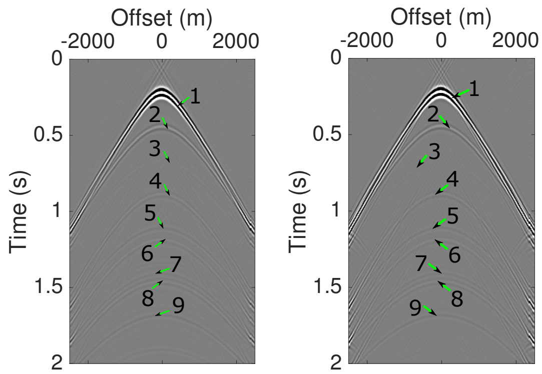

(a) (b)

Figure 4: Downward responses obtained by PSF inversion according to equation (11) with different values of ε: (a) 0.1% and (b) 0.01%.

In a corresponding way, we used the one-way reciprocity theorem of convolution type, equation (10), to retrieve the upgoing Green's functions $\hat{G}^B_-(x', \omega; x^B)$ by means of stabilized least-squares inversion (Figure 5). We observe that, as desired, only the upgoing Green's functions constituents were retrieved. A comparison to Figure 3a reveals correct positioning. Also the dynamic properties of the inverted events correspond well to those in the modelled section.

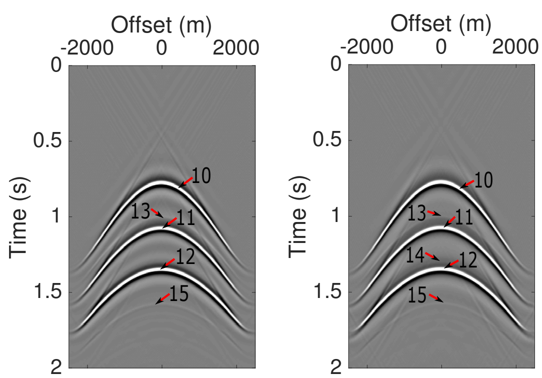

(a) (b)

Figure 5: Upward responses obtained by PSF inversion according to equation (10) with different values of ε: (a) 0.1% and (b) 0.01%.

Finally, Figure 6 shows the source-receiver redatumed wavefields at the datum, recovered by inverting equation (12). We observe that the redatumed wavefields recover the desired primary reflection events with slightly different quality. While the larger values of ε do a better job of suppressing artifacts, they also lead to a stronger damping of the desired wavefield at larger offsets and a certain distortion of the wavelet.

The quality of the inversion result as a function of the regularization parameter can be better assessed in Figure 7, which compares the central trace of each redatuming response for four different values of ε to the modeled trace at the same location. While all events are kinematically nicely matched with the exact trace, we notice that with increasing ε, the instabilities decrease but the wavelet distortion increases.

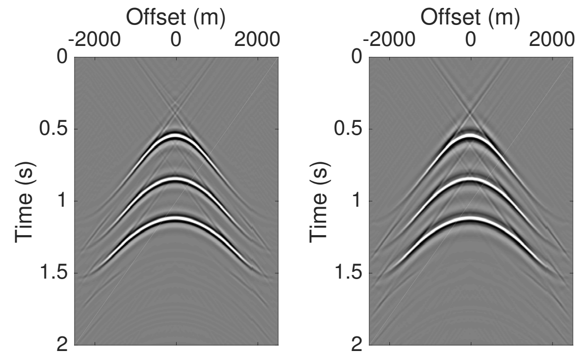

(a) (b)

Figure 6: Redatuming responses with different values of ε in the PSF inversion of equation (12): (a) 0.1% and (b) 0.01%.

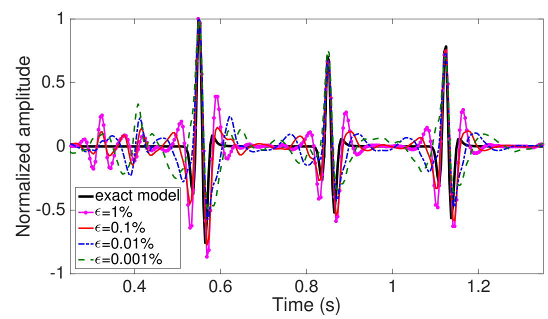

Figure 7: Central traces of the redatuming responses in Figure 6 compared with the central trace of the exact model.

CONCLUSIONS

In this work, we have derived a new interferometric procedure to calculate the down- and upward Green's functions with sources at the earth's surface and receivers at a datum in depth. It makes use of inverse wavefield extrapolation. With this methodology it is possible to retrieve only the down- and upward propagating constituents at an arbitrary focusing surface without anticausal events and without artifacts if the model of the overburden is known.

Combining the down- and upward Green's function retrieved by wavefield inversion with the conventional version of deconvolution-based interferometric redatuming, we were able to retrieve the reflected wavefield at the datum, as demonstrated in a simple synthetic-data example. As a major advantage, there is no influence of anticausal events and no causal interactions with the overburden in the final responses, which were removed with the inverse wavefield extrapolation in the first and second step of the redatuming process.

ACKNOWLEDGMENTS

This work was kindly supported by the Brazilian research agencies CAPES and CNPq as well as Petrobras and the sponsors of the Wave Inversion Technology (WIT) Consortium.